Chemical Engineering Journal 204–206 (2012) 16–22

Contents lists available at SciVerse ScienceDirect

Chemical Engineering Journal

journal homepage: www.elsevier.com/locate/cej

Synthesis of silicate sol–gel matrix embedded silver nanostructures: Efficient nanocatalyst for the reduction of 4-nitrophenol

Shanmugam Manivannan, Bhagavathi Krishnakumari, Ramasamy Ramaraj *

School of Chemistry, Centre for Photoelectrochemistry, Madurai Kamaraj University, Madurai 625 021, India

HIGHLIGHTS

- The single-step synthesis of size-controlled Ag NPs embedded in functionalized amine silicate sol–gel matrix is reported.
- The formation of tetra-twinned Ag NPs is observed in silicate sol–gel matrix.
- The efficient catalytic reduction of 4-nitrophenol in the presence of Ag NPs is observed.

ARTICLE INFO

Article history:
Received 26 April 2012
Received in revised form 6 July 2012
Accepted 20 July 2012
Available online 1 August 2012

Keywords:
Silver nanoparticles
Silicate sol–gel matrix
β-Cyclodextrin
Catalysis
4-Nitrophenol

ABSTRACT

Amine functionalized silicate sol–gel matrix embedded silver nanoparticles (Ag NPs) were prepared in the presence of β-cyclodextrin (β-CD–Ag–TPDT NPs) by a single-step process. The formation of sub-10 nm tetra twinned Ag nanostructures was confirmed by high resolution transmission electron microscopy studies. The reduction of 4-nitrophenol by $NaBH_4$ was used as a model to study the catalytic efficiency of the as prepared Ag nanostructures. The 4-nitrophenol forms an inclusion complex with the hydrophobic β-CD cavity because of the strong affinity of β-CD to the phenyl ring moieties. The catalytic reduction of 4-nitrophenol included in the β-CD cavity by $NaBH_4$ was monitored in the presence of the Ag NPs using the absorption spectrophotometer by the kinetic mode analysis. The catalytic performance of the β-CD–Ag–TPDT NPs was greatly enhanced towards the 4-nitrophenol reduction reaction. The tetra twinned shaped β-CD–Ag–TPDT NPs with the size of sub-10 nm showed higher catalytic activity than the β-CD–Ag NPs and Ag–TPDT NPs.

1. Introduction

The extraordinary optical properties of noble metal nanoparticles (NPs) have led to significant interest into their potential applications in a diverse range of technologies across all scientific fields [1]. Among the noble metal NPs, the Ag NPs have attracted large research efforts as their properties strongly depend on their size [2–4], shape [5], surrounding medium [6], and aggregation state [7]. In particular, the Ag NPs have been extensively investigated because of their optical properties that result from the characteristic absorption bands in the electronic spectra due to the surface plasmon resonance (SPR) [8–11]. The Ag NPs play an important role as substrates in the fields of catalysis [12], photographic processes [13] and surface-enhanced Raman scattering [14] and also find their extensive applications in the field of antimicrobial effects [15], optical and catalytic properties [16].

In recent years, the fabrication of composite materials consisting of polymer matrix encapsulated metal particles has attracted much attention. It is now well-established that the polymer matrices are excellent host materials for metal NPs and semiconductors [17–20]. When the NPs are embedded in a polymer matrix, it acts as a surface capping agent, controlling the size of the NPs well within the desired regime and the casting of film becomes easier which would find extensive applications in the field of chemically modified electrodes [21–26]. To control the size of the metal NPs, usually the NPs dispersed in liquid or solid medium or embedded in polymer matrix are considerably more stable against aggregation/agglomeration [27,28]. The supramolecular structured hydrogels based on the inclusion complex formation of cyclodextrins (CDs) with a variety of host molecules have been widely studied because of the fact that CD as the host molecule is water soluble and capable of selectively including a wide range of guest molecules by their internal hydrophobic cavities [29,30].

We have chosen amine functionalized silicate sol–gel (SSG) matrix–β-CD composite (β-CD–SSG) in aqueous medium as a reducing agent as well as stabilizer for the reduction of Ag precursor to Ag NPs (β-CD–Ag–TPDT NPs). The stabilization of metal NPs in SSG based matrices provides a promising approach to benefit from the advantages of nano-crystalline dispersions for optical, catalytic,

* Corresponding author.
E-mail address: ramarajr@yahoo.com (R. Ramaraj).

1385-8947/$ - see front matter © 2012 Elsevier B.V. All rights reserved.
http://dx.doi.org/10.1016/j.cej.2012.07.092

and electrochemical applications. Another important issue for improving the methods for the preparation of nanomaterials is to develop a green synthesis approach. The use of an aqueous medium for the surfactant directed growth technique is in accordance with the principles of green chemistry. A further step to a greener process will be the replacement of $NaBH_4$ and alkyltrimethylammonium halides by biocompatible agents. In this respect, SSG and CDs as the greener alternative to $NaBH_4$ and alkyltrimethylammonium halide were used for synthesizing Ag nanostructures. Phenol and substituted phenols are known to be present in natural and industrial waste mostly from petroleum, gas, wood, textile, pharmaceutical, papermaking, explosives, insecticide and dyestuff industries. The toxicity of these compounds has been well understood by humans, animals, and plants. In particular 4-nitrophenol is one of the nitrophenols listed in the U.S. Environmental Protection Agency List of Priority Pollutants [31,32]. The monitoring of nitrophenols is a matter of concern for environment control. In our previous report we have studied the catalytic reduction of 4-nitrophenol using the Au NPs embedded in a mesoporous organic gel [33], Kuan et al. used $Ag@Fe_2O_3$ NPs [34], Pal and his coworkers have studied the Ag and Au based nanocomposites for the catalytic reduction of 4-nitrophenol [35–37] and Au based nanocages, nanoboxes and spherical NPs were also subjected to the same [38]. The Au NPs@ZnO [39] and TiO_2/kaolinite composites [40] were used for the degradation of the 4-nitrophenol.

Herein we report a single-step synthesis of Ag NPs using silicate sol–gel and β-CD composite. We have used different amine and methyl functionalized silanes to prepare Ag NPs in the presence of β-CD. The role of TPDT SSG matrix – β-CD composite on the Ag NPs synthesis was analyzed. The colloidal metal NPs stabilized by functionalized silicate sol–gel and its composite with CDs may play a major role in catalysis. The stability of the metal NPs can be improved by using amine functionalized silicate sol–gel matrix [23,41,42]. In the present work, a new approach is attempted to synthesize the amine functionalized silicate sol–gel and its composite with β-CD stabilized Ag NPs and studied their catalytic application.

2. Experimental section

2.1. Materials

Silver nitrate, β-cyclodextrin, *N*-[3-(trimethoxysilyl)propyl] diethylenetriamine (TPDT), *N*-[3-(trimethoxysilyl) propyl] ethylenediamine (EDAS), (3-aminopropyl) triethoxysilalne (APS) and triethoxymethylsilane (ETMOS) were received from Sigma-Aldrich. 4-Nitrophenol (thrice re-crystallized prior to use) and $NaBH_4$ were received from Merck. All glassware were thoroughly cleaned with aqua regia (3:1 HNO_3/HCl (v/v) (*Aqua regia is a powerful oxidizing agent, and it should be handled with extreme care.*) and rinsed extensively with doubly distilled water before use.

2.2. Synthesis of core/shell β-CD–Ag–TPDT NPs

The Ag NPs stabilized by different SSG matrix were synthesized by the following procedure. In a typical experiment, 25 μL of 1 M silane monomer was added to the 5 mL aqueous solution of 7 mM β-CD under vigorous stirring and it was continued for another 60 min to obtain a homogeneous β-CD–SSG matrix composite. To this 50 μL of 0.1 M $AgNO_3$ was added and the mixture was kept stirred for 24 h. The observation of a bright yellow color (for TPDT silane) confirmed the formation of the SSG matrix encapsulated Ag NPs. For the formation of Ag NPs, a light yellow color was observed in EDAS silane, light yellow color followed by aggregation was observed in APS silane and no color change was observed in MTMOS silane.

2.3. Characterizations

Absorption spectra of all samples were recorded on Agilent Technologies 8453 spectrophotometer using 1 cm quartz cell. Water was used as reference sample to record the absorption spectra of the Ag NPs. The shape, size and particle distribution of the β-CD–Ag–TPDT NPs were studied using high resolution transmission electron microscopy (HRTEM) and selected area electron diffraction (SAED) using a JEOL 3010 instrument. The sample was prepared by placing a drop of Ag NPs on a copper grid and then evaporating the solvent under vacuum.

2.4. Catalytic studies

The reduction of 4-nitrophenol by $NaBH_4$ was studied as a model system to probe the catalytic activity of the β-CD–Ag–TPDT NPs in a homogeneous system. Under similar experimental condition, in the absence of a catalyst the 4-nitrophenol reduction did not progress with only $NaBH_4$. To study the reaction, 2 mL of pre-stirred mixture of 4-nitrophenol (7.0×10^{-5} M) and $NaBH_4$ (4.2×10^{-2} M, freshly prepared) in aqueous solution was taken in a quartz cuvette with an optical path length of 1 cm and then 100 μL of the Ag NPs catalyst was added. Immediately after the addition, the UV–visible absorption spectrum was recorded at an interval of 5 s (kinetics mode) to monitor the changes in the reaction mixture. To confirm the catalytic activity of the β-CD–Ag–TPDT NPs, controlled experiments were carried out using only a TPDT SSG matrix (Ag–TPDT) or a β-CD stabilized Ag NPs (β-CD–Ag NPs) under similar experimental condition.

3. Results and discussion

3.1. Spectral studies

The Ag NPs were prepared by mixing $AgNO_3$ and TPDT silane (Ag–TPDT NPs). In another experiment the Ag NPs were prepared by mixing $AgNO_3$ and TPDT silane–β-CD composite (β-CD–Ag–TPDT NPs). The reaction mixture was stirred for 24 h till the formation of the Ag NPs was complete. The SPR absorption spectra recorded for the TPDT matrix embedded Ag NPs in the presence

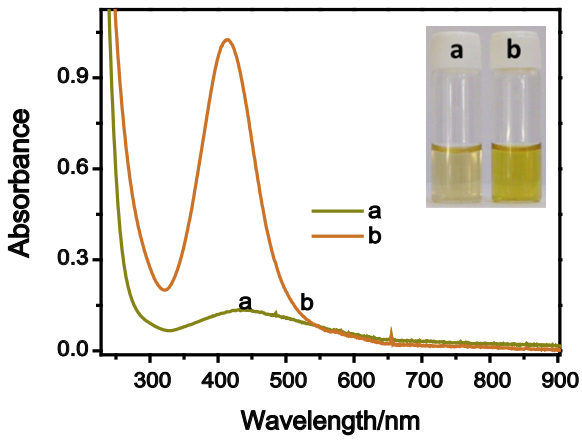

Fig. 1. Surface plasmon absorption spectra obtained for Ag–TPDT NPs (in the absence of β-CD) (a) and β-CD–Ag–TPDT NPs (in the presence of β-CD) (b). Reaction time was 24 h under stirring. Inset shows the photograph of the Ag–TPDT NPs (a) and β-CD–Ag–TPDT NPs.

(Fig. 1b) and absence (Fig. 1a) of β-CD showed absorption maxima at 430 nm and 409 nm, respectively. The observed blue shift of 20 nm in the SPR band (Fig. 1b) for the β-CD–Ag–TPDT NPs suggests that the size of the Ag NPs has decreased to smaller size when compared to the Ag–TPDT NPs (in the absence of β-CD). The efficient reduction of the Ag^+ ions and stabilization of the Ag NPs were observed in the presence of the β-CD–TPDT composite. Previous reports [43,44] show that the alkaline medium facilitates the deprotonation of the β-CD (pH = 4.86) and promotes the kinetic evolution and stabilization of metal NPs. In the present study, when an aqueous solution of the β-CD (pH = 4.86) and TPDT silane (pH = 9.72) were mixed, the pH of the solution changed to 9.84. The TPDT silane on hydrolysis forms silanol (Si–OH) and interacts with the –OH group of the β-CD. At the basic pH, the formation of the deprotonated β-CD (nucleophile) induces the efficient reduction of the Ag^+ ions into Ag NPs. In the absence of β-CD, the triamine group present in the TPDT contributes to the reduction and stabilization process [41,42,45,46]. The reduction of the Ag^+ ions by TPDT is very slow or poor when compared to that by β-CD–TPDT composite. Fig. 1b shows the absorption spectrum recorded after the growth of the Ag NPs in the presence of β-CD whereas the formation was found to be very slow and incomplete in the absence of β-CD (Fig. 1a). Fig. S1 shows the SPR absorption spectra were recorded for the CD–Ag–TPDT NPs prepared using α-CD (a), β-CD (b) and γ-CD (c) under similar experimental conditions (Fig. S1). The complete formation of Ag NPs was observed in the presence of β-CD when compared to α-CD and γ-CD and hence the β-CD was chosen to prepare the β-CD–Ag–TPDT NPs. The absorption spectra obtained for TPDT SSG matrix (a), β-CD (b), and β-CD–TPDT composite (c) without Ag NPs did not show the characteristic band due to the Ag NPs (Fig. S2).

3.2. Role of amine groups in the silanes

To understand the role of different functional groups present in the MTMOS, APS, EDAS and TPDT SSG on the preparation of Ag NPs, the SPR absorption spectra of the different Ag NPs prepared in the presence of four different SSG matrices were recorded and are shown in Fig. 2. It was observed that the reduction of the Ag^+ ions did not take place in the presence of the ETMOS matrix (methyl functionalized) and the absorption band due to the formation of Ag NPs was not observed (Fig. 2a). However, a band was observed at 265 nm due to the β-CD.

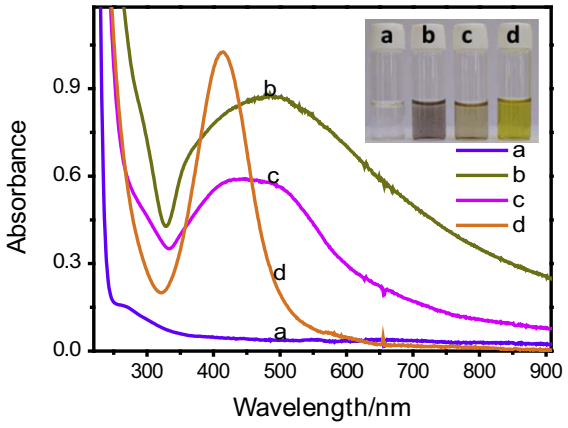

Fig. 2. Surface plasmon absorption spectra obtained for β-CD–Ag–SSG NPs in the presence of ETMOS (a), APS (b), EDAS (c) and TPDT (d) silane monomer reaction time was 24 h under stirring. Inset shows the photograph of the β-CD–Ag–SSG NPs prepared using four different amine functionalized silanes (a–d).

In the presence of APS and EDAS SSG matrices (Fig. 2b and c), the color of the solution turned to light yellow with a band around 400–430 nm in the absorption spectrum and the so formed Ag NPs were not stable. However, the TPDT SSG matrix led to the faster growth of Ag NPs within 24 h (Fig. 2d).

Inset shown in Fig. 1 represents the photograph of the Ag NPs prepared in the absence (a) and presence (b) of β-CD along with TPDT SSG matrix, respectively. The development of intense yellow color was observed in the presence of β-CD (insets b and c) and light yellow color was observed in the absence of β-CD (inset 1a). However, a complete formation of Ag NPs in the absence of the β-CD was observed after 5 days confirming the slow reduction of the Ag^+ ions by TPDT. Inset in Fig. 2 depicts the photograph taken after 24 h for the Ag NPs in the presence of ETMOS, APS, EDAS and TPDT along with the β-CD. Among the four different SSG matrices, in the presence of TPDT SSG matrix an intense yellow color was observed which shows the complete reduction of the Ag^+ ions in the presence of TPDT when compared to the other three SSG matrices.

The observed SPR absorption band maxima of 483,442 and 409 nm for the β-CD–Ag–APS, β-CD–Ag–EDAS and β-CD–Ag–TPDT, respectively is attributed to the following reasons. The presence of APS and EDAS may lead to the formation of anisotropic and aggregated Ag NPs (Fig. 2, inset b). Lev and co-workers [41,42] reported the preparation of noble metal NPs using the amine functionalized APS and EDAS sol–gel matrix. They have concluded that, among the two aminosilanes, EDAS (di-amine) sol was more stable due to the stronger binding (by the two amine groups) to the gold NPs surface than the APS (mono-amine). In the present work, three different amine functionalized (APS (mono-amine), EDAS (di-amine) and TPDT (tri-amine)) silanes along with β-CD were used for the preparation of Ag NPs and the observations revealed that the Ag NPs prepared in the presence of β-CD–TPDT composite showed a narrow absorption band due to the Ag NPs (Fig. 2d) and the Ag NPs were stable for more than 6 months. However, the Ag NPs prepared in the presence of APS and EDAS along with β-CD showed a broad absorption bands and they were also not stable after 1–3 days. Based on this observation, the Ag NPs prepared in the presence of β-CD–TPDT composite was chosen for further studies. Hence, the increase in the number of amine groups in the aminosilane leads to the efficient reduction of Ag^+ ions and increase the stability of Ag NPs.

3.3. Characterization of the Ag NPs

The SEM-EDX and XRD analysis were carried out to confirm the formation of Ag NPs. The SEM-EDX analysis confirmed the presence of elemental Ag (Ag NPs) (Fig. S3). The XRD pattern of the β-CD–Ag–TPDT NPs (Fig. S4) displayed peaks corresponding to (111), (200), and (220) planes of the face-centered cubic lattice and other peaks corresponding to (100), (101), and (104) planes of the primitive hexagonal lattice of Ag NPs. The XRD pattern (Fig. S4) matches with the values of Ag in the JCPDS database (PDF2 Numbers 40783 and 411402). The morphology of the so prepared β-CD–Ag–TPDT NPs were studied by recording the HRTEM images as shown in Figs. 3 and 4. The average particle size was calculated as ~6.1 nm. It is interesting to note that the sub-10 nm Ag NPs with tetra twinned morphology were observed in the β-CD–TPDT composite. The encapsulation of Ag NPs by the TPDT SSG matrix as shell was observed from the contrast difference in the images as dark and bright regions, respectively (Fig. 3A). The d-spacing values calculated from the lattice resolved image (Fig. 4A) corresponds to the (111) and (104) planes of the Ag NPs. Fig. 4B shows the SAED pattern of the β-CD–Ag–TPDT NPs and the calculated crystal plane values ((111), (200), (220), (222) and (311) plane) of the Ag NPs are consistent with the standard JCPDS data base values.

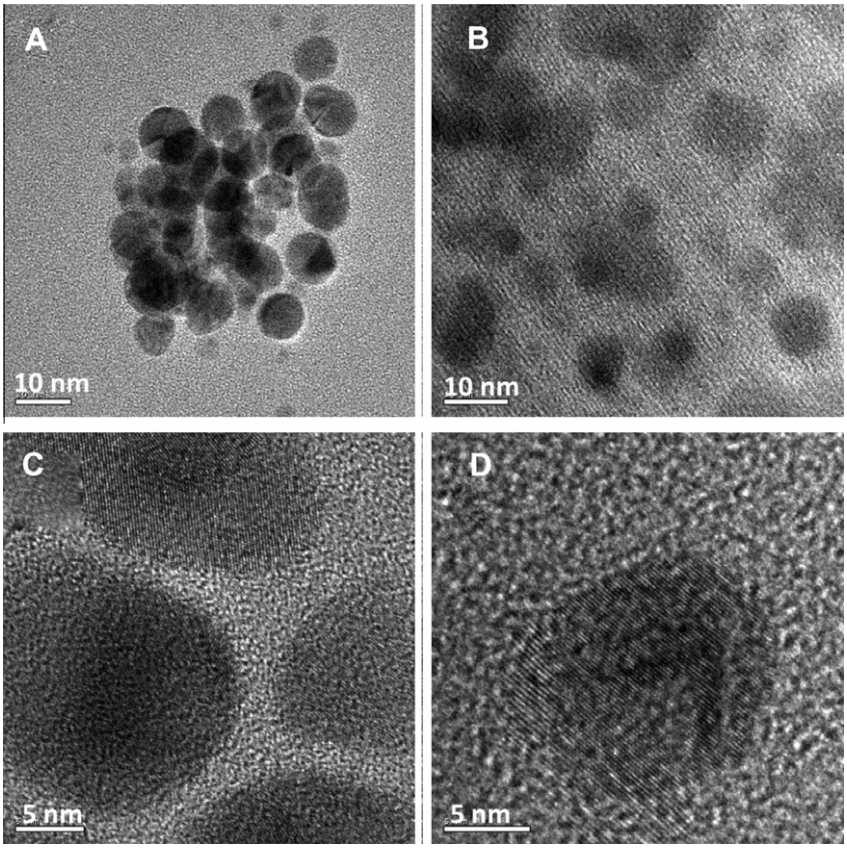

Fig. 3. HRTEM images of Ag–TPDT NPs (A and C) and β-CD–Ag–TPDT NPs (B and D) at different magnifications.

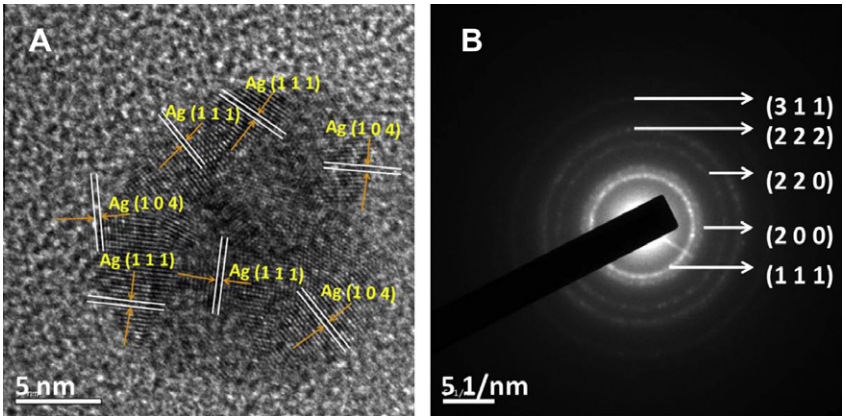

Fig. 4. Lattice resolved HRTEM images of tetra twinned β-CD–Ag–TPDT NPs (A) and the SAED pattern (B).

3.4. Role of β-CD and pH on the formation of Ag NPs

During the formation of Ag NPs, the deprotonated primary alcoholic groups present in β-CD undergo oxidation at basic condition and the secondary alcoholic groups in β-CD do not undergo oxidation [47,48]. Luong and co-workers [49–51] broadly discussed the interaction involved between the Au NPs and β-CD leading to the formation of smaller size Au NPs in the presence of the β-CD. According to them, the reduction of $HAuCl_4$ in aqueous solution leads to the formation of partially hydroxylated surface (Au–OH, $pK_a = 3.2$). Effective hydrogen bonding between the Au NPs and the β-CD is possible only when $-O^-$ groups are present on the Au NPs surface. The same mechanism can be adapted to the synthesis of β-CD–Ag–TPDT NPs. When TPDT silane and β-CD are introduced in the solution, β-CD would exhibit hydrophobic interaction with the embryonic Ag NPs and hence the consecutive particle growth due to the mutual coalescence among the nanoclusters would be severely limited which leads to the formation of smaller Ag NPs. The rapid reduction of the metal precursor leads to the quick agglomeration of the nucleation centers and results in the formation of larger particle size. In the presence of β-CD, mutual coalescence among nucleation centers is restricted by means of providing its cavity as nanocages for NPs growth [51] and thus ultimately the particle size is reduced. Considering the Ag NPs size and the β-CD cavity size, the inclusion of fully grown Ag NPs into the cavity of the β-CD is ruled out. Therefore, the formation of sub-10 nm Ag

NPs in the presence of β-CD is attributed to the hydrophobic interactions between the β-CD and Ag NPs rather than the inclusion of small Ag NPs into the β-CD cavities. Considering the interaction between the TPDT SSG matrix and β-CD in the β-CD–TPDT composite, the hydrogen present in the amine groups is acidic and hydrophilic in nature and the inclusion of the chain into the β-CD cavity may be restricted due to the weak interaction between TPDT and β-CD. Hence, the strong host–guest interaction between β-CD and TPDT SSG matrix is not expected. However, the Ag NPs formed in the presence of APS SSG matrix–β-CD composite (Fig. 2b and inset b) gets aggregated and such aggregation is not observed in the case of EDAS or TPDT SSG matrix–β-CD composites.

The pH of the reaction mixture plays a crucial role in the reduction of Ag^+ ions in the presence of β-CD–TPDT composite. It can be considered that the lack of deprotonation in the β-CD (pH = 3.41) is the reason for the absence of Ag^+ ions reduction and the formation of Ag NPs [43]. The presence of TPDT alone (pH = 9.52) led to the slow reduction of Ag^+ ions due to the presence of tri-amine groups in the TPDT. When β-CD (pH = 4.86) was mixed with TPDT silane (pH = 9.72) deprotonation of β-CD occurred and effective reduction of Ag^+ ions into Ag NPs was observed at the pH of 9.59. The amine functionalized TPDT silane undergoes hydrolysis to form silicate sol–gel and then homogeneous β-CD–TPDT composite with pH 9.72 and at this basic pH the Ag NPs formation occurred.

3.5. Catalytic reduction of 4-nitrophenol

The β-CD–Ag–TPDT NPs assisted catalytic reduction of 4-nitrophenol in the presence of $NaBH_4$ was used as a model system to evaluate the catalytic activity of the β-CD–Ag–TPDT NPs. The experimental method was described in the experimental section. Previous reports [33–40] reveal that the 4-nitrophenol reduction reaction is catalyzed by the metal NPs and semiconductor nanocomposites and the color changes involved during the reduction reaction provide a simple way to monitor the reaction kinetics using the spectroscopic method. In neutral or acidic condition, 4-nitrophenol exhibits a strong absorption peak at 317 nm. Upon the addition of $NaBH_4$ to the 4-nitrophenol, the increased alkalinity of the solution leads to the formation of 4-nitrophenolate ions with a new absorption band at 400 nm [52,53].

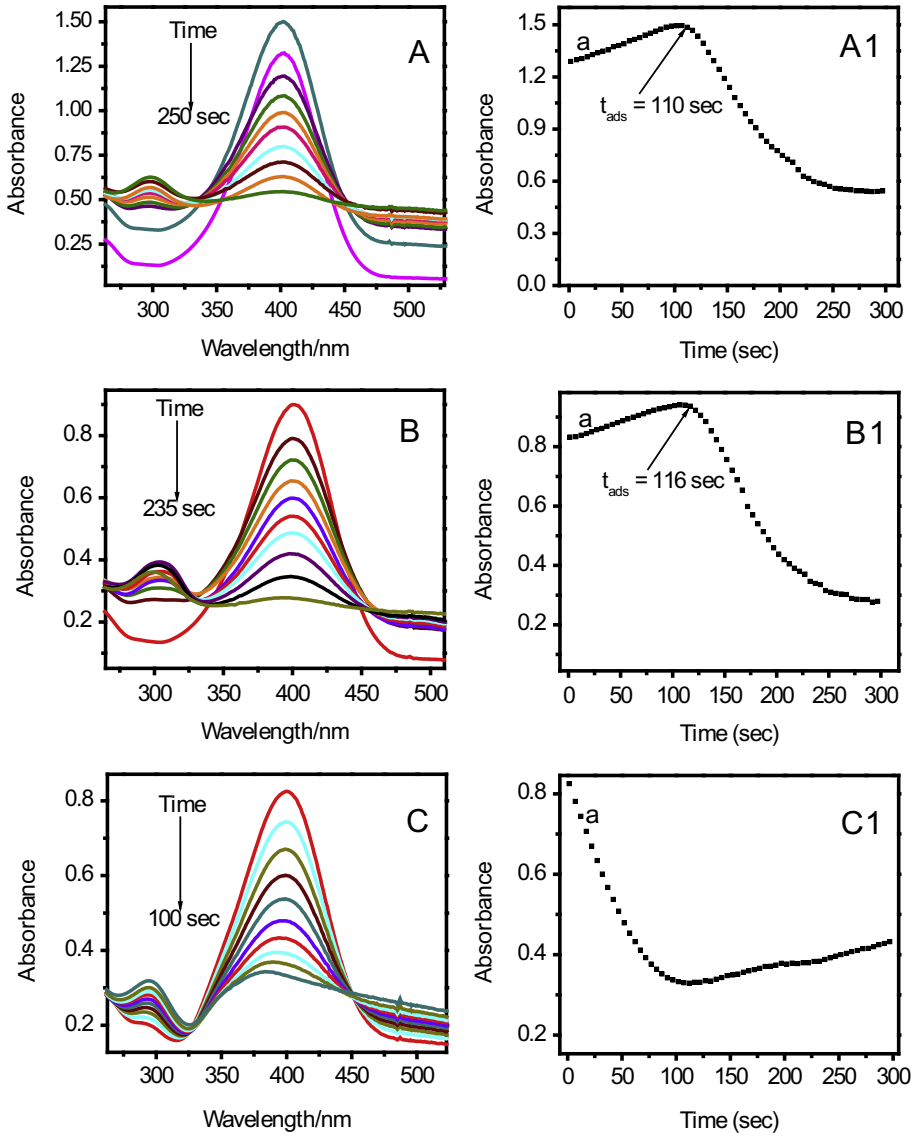

Fig. 5. Absorption spectra observed at different reaction time indicating the decrease in the absorbance intensity at 400 nm and the appearance of a new band at 297 nm due to the 4-nitrophenolate ion reduction to $-NH_2$ upon the addition of β-CD (A), β-CD–Ag (B) and β-CD–Ag–TPDT NPs (C) into the mixture of 4-nitrophenol and $NaBH_4$. Corresponding plots of absorbance at 400 nm against time (A1–C1). In all the cases, the concentrations of 4-nitrophenol and $NaBH_4$ were 7.0×10^{-5} and 4.2×10^{-2} M, respectively. 100 μL of Ag NPs catalyst was added to 2 ml of reaction mixture.

Upon the addition of β-CD–Ag–TPDT NPs to the mixture of 4-nitrophenol and $NaBH_4$ the absorption band at 400 nm due to the 4-nitrophenoalte ion gradually decreased as the catalytic reduction reaction proceeded. The catalytic reduction of 4-nitrophenolate ion led to the formation of a new band at 297 nm due to the formation of 4-aminophenol. Fig. 5C represents the β-CD–Ag–TPDT NPs assisted catalytic reduction of 4-nitrophenol in the presence of $NaBH_4$. Hence, the decrease in the concentration of 4-nitrophenolate ions was monitored by recording the absorbance at 400 nm for every 5 s. In all the experiments, the initial concentration of 4-nitrophenol and $NaBH_4$ were kept as 7.0×10^{-5} and 4.2×10^{-2} M, respectively. Fig. S5 shows the absorption spectra for the 4-nitrophenol was recorded in the presence of β-CD and $NaBH_4$. In this case, since the solution turned to basic (pH = 9.21) the formation of 4-nitrophenolate ion was observed at 400 nm (Fig. S5b). Upon the addition of β-CD to the 4-nitrophenol (solution pH = 5.51), the reduction of 4-nitrophenol was not observed. Since the solution pH was 5.51, the deprotonation of the 4-nitrophenol did not occur (pK_a of 4-nitrophenol is 7.15) and hence the absorption band at 317 nm for 4-nitrophenol was not shifted to 400 nm (Fig. S5a). In both the cases, the absorbance with time did not change. This result indicates that the reduction of 4-nitrophenol was not taking place only in the presence of β-CD.

Interestingly, the addition of β-CD to 4-nitrophenol in the presence of $NaBH_4$ led to the slow reduction of 4-nitrophenol even in the absence of the Ag NPs catalyst (Fig. 5A). However, the formation of the inclusion complex between 4-nitrophenol and β-CD occurred first and the reduction proceeded after 110 s (t_{ads}), (t_{ads} called time of adsorption). Then a slow decrease in the absorbance of 4-nitrophenolate ions at 400 nm was observed. However, the reduction of 4-nitrophenol by β-CD was not observed in the absence of $NaBH_4$. Fig. 5B shows the absorption spectral changes observed upon the addition of β-CD stabilized Ag NPs (β-CD–Ag NPs) to the solution of 4-nitrophenol and $NaBH_4$. For this system, the t_{ads} was observed as 116 s and then the reduction reaction occurred. When the Ag–TPDT NPs were added to the reaction mixture the reduction reaction was not observed (data not given). This means that the β-CD stabilized Ag NPs catalyzed the reduction reaction by forming an inclusion complex with 4-nitrophenalate ion. To confirm the influence of β-CD–TPDT composite material on the reduction process, the Ag–TPDT NPs was used as catalyst for the reduction process and the spectral change due to the formation of 4-aminophenol was not observed. This observation confirms that the β-CD–Ag–TPDT NPs catalyzed the reduction of 4-nitrophenol to 4-aminophenol. When the β-CD–Ag–TPDT SSG NPs were introduced in the presence of $NaBH_4$, faster reduction was observed and the reaction was over in 100 s as shown in Fig. 5C. The considerable enhancement in the catalytic activity of the β-CD–Ag–TPDT NPs is probably to be attributed to the following: β-CD forms an inclusion complex with 4-nitrophenol and facilitates the electron transfer from BH_4^- ions (donor) to 4-nitrophenolate ions (acceptor) upon the addition of β-CD–Ag–TPDT NPs. It is worth mentioning that, upon the addition of β-CD–Ag–TPDT NPs catalyst in the presence of $NaBH_4$, a decrease in the intensity at 400 nm along with the developing of a new band at 297 nm due to the formation of 4-aminophenol was observed and this process was over in 100 s (Fig. 5C). Further, a isobestic point was observed in the absorption spectra during the reduction of 4-nitrophenol which confirms the formation of 4-aminophenol.

The comparison of plots of absorption at 400 nm against time for the reduction of 4-nitrophenol using four different catalyst systems showed that the reduction reaction catalyzed by β-CD–Ag–TPDT NPs was the fastest one (Fig. S6). In order to understand the influence of $NaBH_4$, β-CD, TPDT SSG matrix and β-CD–TPDT composite, controlled experiments were performed and the plots of absorbance at 400 nm against time for the reduction of 4-nitrophenol are shown in *Fig.* S7. It is observed that the TPDT SSG matrix (Fig. S7a), β-CD–TPDT composite (Fig. S7b) and the β-CD–Ag–TPDT NPs in the absence of $NaBH_4$ (*Fig.* S7e) did not show any effect on the 4-nitrophenol reduction process. Interestingly, the reaction occurred in the presence of $NaBH_4$ only when β-CD was added into the reaction mixture (Fig. 5A). The reduction reaction occurred faster when the β-CD–Ag–TPDT NPs were added (Fig. S7d). It is observed that from the controlled experiments (Fig. S7a and b) that the TPDT or β-CD–TPDT composite (in the absence of Ag NPs) or Ag–TPDT NPs does not act as a catalyst for the reduction of 4-nitrophenol in the presence of $NaBH_4$. However, the addition of β-CD alone (without Ag NPs) in the presence of $NaBH_4$ reduces the 4-nitrophenol (Fig. S7c). In the case of β-CD, the catalytic reduction of 4-nitrophenol occurred after 116 s t_{ads} (Fig. 5B). However, when β-CD–Ag–TPDT NPs was used as a catalyst the 4-nitrophenol reduction occurred without t_{ads}. In this case (β-CD–Ag–TPDT NPs), the β-CD cavity may not be free and forms composite with TPDT and the composite interacts with the Ag NPs and t_{ads} was not observed (Fig. 5C). Furthermore, the actual effect observed in the presence of β-CD–Ag–TPDT NPs is due to the synergistic effect of β-CD, TPDT and Ag NPs. In conclusion, the presence of β-CD and the size of Ag NPs play a crucial role in the catalytic reduction of 4-nitrophenol.

4. Summary

A single-step synthesis of TPDT SSG matrix embedded Ag NPs in the presence of β-CD was reported. The role of the SSG matrix and the β-CD composite towards the Ag NPs synthesis were analyzed. The formation of tetra twinned Ag NPs was confirmed by HRTEM studies. The stability and the catalytic effect of Ag NPs were improved when β-CD–TPDT composite (TPDT) (tri-amine) was used to prepare the Ag NPs. The reduction of 4-nitrophenol in the presence of $NaBH_4$ was used as a model to study the catalytic effect of as prepared β-CD–Ag–TPDT NPs. The results showed better catalytic performance for the β-CD–Ag–TPDT NPs when compared to the β-CD molecules, β-CD–Ag NPs and Ag–TPDT NPs. The tetra twinned shaped with the size of sub-6 nm β-CD–Ag–TPDT NPs showed higher catalytic activity than β-CD stabilized Ag NPs.

Acknowledgements

RR acknowledges the financial support from the Department of Science and Technology (DST), New Delhi. SMV is a recipient of a CSIR-Senior Research Fellowship. The HRTEM images were recorded at the IIT Madras, Chennai.

Appendix A. Supplementary material

Supplementary data associated with this article can be found, in the online version, at http://dx.doi.org/10.1016/j.cej.2012.07.092.

References

[1] K.A. Willets, R.P. Van Duyne, Localized surface plasmon spectroscopy and sensing, Annu. Rev. Phys. Chem. 58 (2007) 267–297.
[2] J. Zheng, P.R. Nicovich, R.M. Dickson, Highly fluorescent noble-metal quantum dots, Annu. Rev. Phys. Chem. 58 (2007) 409–431.
[3] C.M. Aikens, S.Z. Li, G.C. Schatz, From discrete electronic states to plasmons: TDDFT optical absorption properties of Ag_n ($n = 10, 20, 35, 56, 84, 120$) tetrahedral clusters, J. Phys. Chem. C 112 (2008) 11272–11279.
[4] K.L. Kelly, E. Coronado, L.L. Zhao, G.C. Schatz, The optical properties of metal nanoparticles: the influence of size, shape, and dielectric environment, J. Phys. Chem. B 107 (2003) 668–677.
[5] M. Hu, J.Y. Chen, Z.Y. Li, L. Au, G.V. Hartland, X.D. Li, M. Marquez, Y.N. Xia, Gold nanostructures: engineering their plasmonic properties for biomedical applications, Chem. Soc. Rev. 35 (2006) 1084–1094.

[6] A. Moores, F. Goettmann, The plasmon band in noble metal nanoparticles: an introduction to theory and applications, New J. Chem. 30 (2006) 1121–1132.
[7] H. Wang, D.W. Brandl, P. Nordlander, N.J. Halas, Plasmonic nanostructures: artificial molecules, Acc. Chem. Res. 40 (2007) 53–62.
[8] J. Dai, M.L. Bruening, Catalytic nanoparticles formed by reduction of metal ions in multilayered polyelectrolyte films, Nano Lett. 2 (2002) 497–501.
[9] D. Zhang, L. Qi, J. Ma, H. Cheng, Formation of silver nanowires in aqueous solutions of a double-hydrophilic block copolymer, Chem. Mater. 13 (2001) 2753–2755.
[10] I.P. Santos, L.M. Marzan, Formation and stabilization of silver nanoparticles through reduction by *n*,*n*-dimethylformamide, Langmuir 15 (1999) 948–951.
[11] A. Manna, T. Imae, K. Aoi, M. Okada, T. Yogo, Synthesis of dendrimer-passivated noble metal nanoparticles in a polar medium: comparison of size between silver and gold particles, Chem. Mater. 13 (2001) 1674–1681.
[12] A. Manna, T. Imae, M. Iida, N. Hisamatsu, Formation of silver nanoparticles from a *n*-hexadecylethylenediamine silver nitrate complex, Langmuir 17 (2001) 6000–6004.
[13] Y.P. Sun, J.E. Riggs, H.W. Rollins, R. Guduru, Strong optical limiting of silver-containing nanocrystalline particles in stable suspensions, J. Phys. Chem. B 103 (1999) 77–82.
[14] T. Sun, K. Seff, Silver clusters and chemistry in zeolites, Chem. Rev. 94 (1994) 857–870.
[15] S. Shanmugam, B. Viswanathan, T.K. Varadarajan, A novel single step chemical route for noble metal nanoparticles embedded organic–inorganic composite films, Mater. Chem. Phys. 95 (2005) 51–55.
[16] W.C. Lin, M.C. Yang, Novel Silver/poly(vinyl alcohol) nanocomposites for surface-enhanced Raman scattering-active substrates, Macromol. Rapid Commun. 26 (2005) 1942–1947.
[17] Z.M. Mbhele, M.G. Sakmane, C.G. Sittert, J.M. Nedeljkovic, V. Djokovic, A.S. Luyt, Fabrication and characterization of silver–polyvinyl alcohol nano-composites, Chem. Mater. 15 (2003) 5019–5024.
[18] G.D. Liang, S.P. Bao, S.C. Tjong, Microstructure and properties of polypropylene composites filled with silver and carbon nanotube nanoparticles prepared by melt-compounding, Mater. Sci. Eng. B 142 (2007) 55–61.
[19] Z. Zhang, M. Han, One-step preparation of size-selected and well-dispersed silver nanocrystals in polyacrylonitrile by simultaneous reduction and polymerization, J. Mater. Chem. Commun. 13 (2003) 641–643.
[20] K. Mullick, M.J. Witcomb, M.S. Scurrell, Polymer stabilized silver nanoparticles: a photochemical synthesis route, J. Mater. Sci. 39 (2004) 4459–4463.
[21] W.K. Yong, L.D. Kyoung, J.L. Kyung, R.M. Byoung, H.K. Jong, *In situ* formation of silver nanoparticles within an amphiphilic graft copolymer film, J. Polym. Sci. Part B: Polym. Phys. 11 (2007) 1283–1290.
[22] C.J. Zhao, Q.T. Zhao, Q.Z. Zhao, Preparation and optical properties of Ag/PPy composite colloids, J. Photochem. Photobiol. A 187 (2007) 146–151.
[23] G. Maduraiveeran, R. Ramaraj, Potential sensing platform of silver nanoparticles embedded in functionalized silicate shell for nitroaromatic compounds, Anal. Chem. 81 (2009) 7552–7560.
[24] G. Maduraiveeran, R. Ramaraj, Gold nanoparticles embedded in silica sol–gel matrix as an amperometric sensor for hydrogen peroxide, J. Electroanal. Chem. 608 (2007) 52–58.
[25] S. Manivanan, R. Ramaraj, Core–shell Au/Ag nanoparticles embedded in silicate sol–gel network for sensor application towards hydrogen peroxide, J. Chem. Sci. 121 (2009) 735–743.
[26] G. Maduraiveeran, R. Ramaraj, A facile electrochemical sensor designed from gold nanoparticles embedded in three-dimensional sol–gel network for concurrent detection of toxic chemicals, Electrochem. Commun. 9 (2007) 2051–2055.
[27] B.A. Rozenberg, R. Tenneb, Polymer-assisted fabrication of nanoparticles and nanocomposites, Prog. Polym. Sci. 33 (2008) 40–112.
[28] X. Zhao, L. Lv, B. Pan, W. Zhang, S. Zhang, Q. Zhang, Polymer-supported nanocomposites for environmental application: a review, Chem. Eng. J. 170 (2011) 381–394.
[29] S.P. Zhao, L.M. Zhang, D. Ma, Supramolecular hydrogels induced rapidly by inclusion complexation of poly(ε-caprolactone)–poly(ethylene glycol)–poly(ε-caprolactone) block copolymers with α-cyclodextrin in aqueous solutions, J. Phys. Chem. B 110 (2006) 12225–12229.
[30] S.P. Zhao, L.M. Zhang, D. Ma, C. Yang, L. Yan, Fabrication of novel supramolecular hydrogels with high mechanical strength and adjustable thermosensitivity, J. Phys. Chem. B 110 (2006) 16503–16507.
[31] US Environmental Protection Agency, Fed. Regist. 44 (1979) 233.
[32] US Environmental Protection Agency, Fed. Regist. 52 (1989) 131.
[33] H. Yang, K. Nagai, T. Abe, H. Homma, T. Norimatsu, R. Ramaraj, Enhanced catalytic activity of gold nanoparticles doped in a mesoporous organic gel based on polymeric phloroglucinol carboxylic acid–formaldehyde, Appl. Mater. Interfaces 1 (2009) 1860.
[34] K.S. Shin, J.Y. Choi, C.S. Park, H.J. Jang, K. Kim, Facile synthesis and catalytic application of silver-deposited magnetic nanoparticles, Catal. Lett. 133 (2009) 1–7.
[35] S. Sandip, P. Anjali, K. Subrata, B. Soumen, P. Tarasankar, Photochemical green synthesis of calcium–alginate-stabilized Ag and Au nanoparticles and their catalytic application to 4-nitrophenol reduction, Langmuir 26 (2010) 2885–2893.
[36] P. Narayan, P. Anjali, P. Tarasankar, Silver nanoparticle catalyzed reduction of aromatic nitro compounds, Colloids Surf., A 196 (2002) 247–257.
[37] P. Sudipa, B. Soumen, P. Snigdhamayee, P. Surojit, J. Subhra, P. Anjali, G. Sujitkumar, P. Tarasankar, Synthesis and size-selective catalysis by supported gold nanoparticles: study on heterogeneous and homogeneous catalytic process, J. Phys. Chem. C 111 (2007) 4596–4605.
[38] J. Zeng, Q. Zhang, J. Chen, Y. Xia, A comparison study of the catalytic properties of au-based nanocages, nanoboxes, and nanoparticles, Nano Lett. 10 (2010) 30–35.
[39] H. Koga, T. Kitaoka, One-step synthesis of gold nanocatalysts on a microstructured paper matrix for the reduction of 4-nitrophenol, Chem. Eng. J. 168 (2011) 420–425.
[40] Y. Zhang, H. Gan, G. Zhang, A novel mixed-phase TiO_2/kaolinite composites and their photocatalytic activity for degradation of organic contaminants, Chem. Eng. J. 172 (2011) 936–943.
[41] S. Bharathi, N. Fishelson, O. Lev, Direct synthesis and characterization of gold and other noble metal nanodispersions in sol–gel-derived organically modified silicates, Langmuir. 15 (1999) 1929–1937.
[42] S. Bharathi, M. Nogami, O. Lev, Electrochemical organization of gold nanoclusters in three dimensions as thin films from an aminosilicate-stabilized gold sol and their characterization, Langmuir 17 (2001) 2602–2609.
[43] P. Surojit, K.G. Sujit, P. Snigdhamayee, P. Sudipa, B. Soumen, J. Subhra, P. Anjali, T. Tatsuya, P. Tarasankar, Synthesis of normal and inverted gold–silver core–shell architectures in β-cyclodextrin and their applications in SERS, J. Phys. Chem. C 111 (2007) 10806–10813.
[44] H.B.N. Choon, Y. Jiexiang, Y.F. Wai, Synthesis and self-assembly of one-dimensional sub-10 nm Ag nanoparticles with cyclodextrin, J. Phys. Chem. C 112 (2008) 4141–4145.
[45] O. Lev, M. Tsionsky, L. Rabinovich, V. Glezer, S. Sampath, I. Pankratov, J. Gun, Organically modified sol–gel sensors, Anal. Chem. 67 (1995) 22A–30A.
[46] K. Ramanathan, D. Avnir, A. Modestov, O. Lev, Sol–gel derived ormosil-exfoliated graphite–TiO_2 composite floating catalyst: photodeposition of copper, Chem. Mater. 9 (1997) 2533–2540.
[47] C. Fraschini, M.R. Vignon, Selective oxidation of primary alcohol groups of β-cyclodextrin mediated by 2,2,6,6-tetramethylpiperidine-1-oxyl radical (TEMPO), Carbohydr. Res. 328 (2000) 585–589.
[48] M.E. Deary, D.M. Davies, Evidence for cyclodextrin dioxiranes, Carbohydr. Res. 309 (1998) 17–29.
[49] Y. Liu, K.B. Male, P. Bouvrette, J.H.T. Luong, Control of the size and distribution of gold nanoparticles by unmodified cyclodextrins, Chem. Mater. 15 (2003) 4172–4180.
[50] J.P. Sylvestre, A.V. Kabashin, E. Sacher, M. Meunier, J.H.T. Luong, Stabilization and size control of gold nanoparticles during laser ablation in aqueous cyclodextrins, J. Am. Chem. Soc. 126 (2004) 7176–7177.
[51] K.B. Male, J. Li, C.C. Bun, S.C. Ng, J.H.T. Luong, Synthesis and stability of fluorescent gold nanoparticles by sodium borohydride in the presence of mono-6-deoxy-6-pyridinium-β-cyclodextrin chloride, J. Phys. Chem. C 112 (2008) 443–451.
[52] K. Hayakawa, T. Yoshimura, K. Esumi, Preparation of gold–dendrimer nanocomposites by laser irradiation and their catalytic reduction of 4-nitrophenol, Langmuir 19 (2003) 5517–5521.
[53] S. Praharaj, S. Nath, S.K. Ghosh, S. Kundu, T. Pal, Immobilization and recovery of Au nanoparticles from anion exchange resin: resin-bound nanoparticle matrix as a catalyst for the reduction of 4-nitrophenol, Langmuir 20 (2004) 9889–9892.